

DELFT UNIVERSITY OF TECHNOLOGY

BACHELOR FINAL PROJECT

Wave propagation through a nickel plate

Author:

A.W. DE KATER

Supervisor:

Dr.ir. Martin Rohde

October 3, 2019

TU Delft, Faculty of Applied Sciences, BSc program Applied Physics



1 Abstract

In this report the wave propagation of ultrasonic waves in a nickel plate is discussed. The research's objective is to determine the travel speed and attenuation of ultrasonic waves through a nickel wave guide. The ultrasonic wave propagation through the nickel wave guide could be used to do measurements for the material properties of molten salt used in molten salt nuclear reactors. The values for the wave velocity and attenuation are determined for different plate temperatures. The surface where the waves are induced is also varied. The size of the surface where the waves are induced remains constant, the position of this surface is varied along one end of the plate. The plate dimensions are 20 *mm* by 0.1 *mm* by 40 *mm* in what is referred to as x,y and z direction respectively, with the wave induced at one end of the plate along the z axis. The experiment is done by simulating the behaviour of the waves in a digital model using COMSOL Multiphysics®[1]. This abstract is followed by the introduction which gives the reason for the experiment. After the introduction the theory section 3 explains the moduli of elasticity that are the material properties that govern the wave propagation through a material. Also different types of waves types that occur are described in the theory. In section 4 model which follows the theory the model that is used is explained as well as the method that is used to obtain the desired information from the acquired data. The section model is followed by the results and discussion section 5 where the results from the simulation are listed as well as the uncertainty of the results and the other information that is relevant when considering the results. The conclusion section 6 follows the results and discussion section, this section contains the conclusion of the research as well as advice for future research. The used sources are listed in the references after the conclusion. The references are followed by the appendices that contain the the code used to process the data and a list of the input parameters used for the simulation. as well as data points found in this research.

Contents

1	Abstract	2
2	Introduction	4
3	Theory	7
3.1	Stress	7
3.2	Strain	7
3.3	Moduli of elasticity	9
3.3.1	Young's modulus	9
3.3.2	Shear modulus	9
3.3.3	Bulk modulus	9
3.3.4	Poisson's ratio	10
3.4	Wave types	11
3.4.1	Lamb waves symmetrical	11
3.4.2	Lamb waves asymmetrical	12
3.4.3	Shear waves	12
4	Model	14
4.1	simulation	14
4.1.1	Discretization	14
4.2	Data processing	15
5	Results and Discussion	19
5.1	temperature	19
5.2	transducer location	20
5.3	wave polarization	21
5.4	Displacement measurement	21
5.5	Uncertainty	23
6	Conclusion	30
	References	31
A	Appendix A Matlab code	33
B	Appendix B data	43
C	Appendix C COMSOL Multiphysics® simulation parameters	48

2 Introduction

With the finalization of the dutch climate accord in December of 2018, the goal of reducing the carbon dioxide emission by 49% by 2030 compared to 1990 is set. In order for these goals to be reached great changes in energy production are required[2]. Nuclear energy produces little greenhouse gas when compared to traditional fossil fuel generators and while fossil fuel reserves are becoming less obtainable nuclear fuel is not nearing the problem in the near future [3]. Most nuclear power plants today use light water reactors. These light water reactors generate long living radio active waste furthermore the high pressure used in these reactors can cause an explosion and the reactor has to be shut down for new fuel to be added [4]. Because of these problems with the current nuclear reactors nine country's combined there efforts to design new types of nuclear reactors by forming the Generation IV International Forum (GIF)[5], one of the new concepts for nuclear reactors is the Molten Salt Reactor (MSR) [6]. With molten salt reactors molten salt is used to transfer heat and can also be used to to circulate the reactor fuel. Molten salt reactors like currently in use reactors rely on nuclear fission to produce heat that can be used to generate electrical energy. Nuclear fission is a process where the nucleus of an atom is hit by a neutron causing is to split into multiple smaller parts, materials that can be used for this process are called fissile materials. The neutrons emitted by the fission reaction can be absorbed by certain nuclei without causing a split, this process can be used to bread fissile material from non fissile material [7]. In order to keep a fission reaction going it is important that the fission reaction emits neutrons to bread new fissile material and initiate new fission reactions. The neutrons emitted by fission reactions have to be slowed down in order for the neutrons to be able to initiate new fission reactions [8]. Neutrons are slowed down by moderating materials like water and graphite. Molten salt reactors have moderating materials located at the core, the liquid salt in circulated through the core only causing the fission reactions to happen within the core because of the presence of the moderating material. The circulation also drives the liquid salt past a fuel processing plant and a heat exchange as can be seen in figure 1. The heat exchange transports heat generated by the nuclear reaction to a secondary loop. the heat passes through several more heat exchanges and is eventually used to generate electrical power via a turbine. The fuel processing plant regulates the liquid salt mixture, while the liquid passes through the processing plant new material is added that can be bread into fissile material and reactants from the fission reaction are removed. With most currently in use nuclear reactors there is no liquid fuel mixture which is why it is necessary to stop the reactor every several years in order to restock on the fuel used in these reactors[9].

Molten salt reactors has multiple advantages in terms of safety, one of which is that molten salt reactors can be equipped with a freeze plug. When the fuel of the molten salt reactor is dissolved in the molten salt the reactor can be stopped by draining the molten salt from the core, a container can be placed underneath the reactor to store the drained molten salt. The passage from the reactor to the storage container can be blocked by a

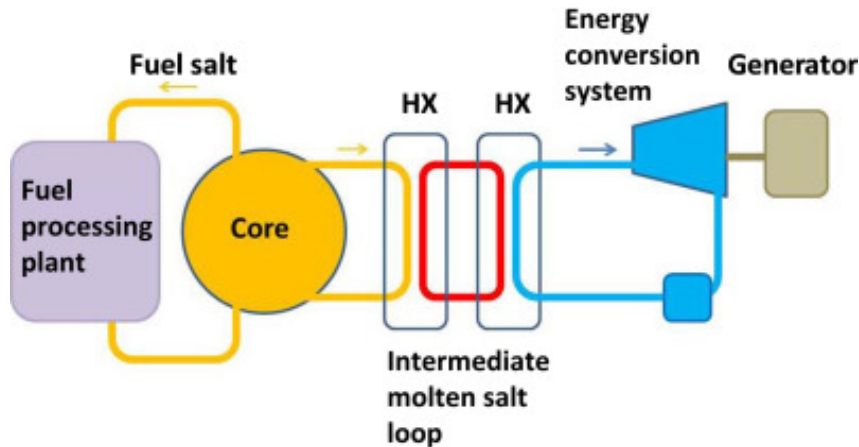


Figure 1: schematic image of a single-fluid liquid fuel reactor

lump of salt. This lump of salt is called the freeze plug [10]. When the freeze plug melts, the molten salt will be drained from the reactor into the storage tank. The freeze plug can melt when the active cooling used to keep the plug solid stops because of a power outage or when the liquid salt gets too hot. The freeze plug will therefore provide extra safety during a power outage, or during other problems that cause the molten salt to get too hot.

Another safety advantage is that molten salt reactors operate at a pressure near atmospheric [11] whereas a conventional nuclear reactor can have pressures of 30 Mpa [12]. This lower operating pressure reduces the risk of a breach in the reactor spreading radioactive material. A disadvantage of the molten salt reactor compared to traditional pressurized water reactors is that the liquid salt can cause corrosion, endangering the integrity of the system [13].

The flow of the molten salt greatly influences the working of the molten salt reactor since the flow of the molten salt is necessary for adequate heat transfer. The flow of the molten salt is influenced by the characteristics of the molten salt like the viscosity and the density. To regulate the heat transferred by the molten salt it is important to know how the molten salt flows, in order to determine the flow of the molten salt the material properties of the molten salt have to be known. A difficulty in measuring the material properties of molten salt is that the equipment used has to be able to withstand the corrosive effects and temperature of the molten salt. A lot of measurement devices used for other liquids are unpractical because of the temperature and corrosive effects of the salt [13]. Ultrasonic waves can help with a great variety of measurements, one of which is measuring the viscosity and density of fluids. The ultrasonic wave viscosity measurements can be used to measure the viscosity of molten salt used in molten salt reactors. Because a wave guide can be used the transducer doesn't have to come in direct contact with the molten salt, however the effect of the wave guide on the wave propagation had to

be taken into account. Acoustics can determine the viscosity and density of a medium because the propagation of the wave is dependent on these factors so analyzing the wave propagation yields the material properties of the medium. In order to analyze the wave propagation, a ultrasonic wave can be directed into the molten salt using a wave guide, the reflection of the wave can be analyzed. by looking at the attenuation and delay the reflected wave has experienced the characteristics of the molten salt can be determined. The effects of the transducer location, the induced wave polarization and the wave-guide temperature are investigated. The temperature is varied because during the start up of the reactor the temperature of the molten salt will increase and the behaviour at these varying temperatures are important to be known. The wave polarization and the location where the waves are induced can be chosen when designing a measurement device. Differences in these factors can influence the attenuation of the wave and thus change the signal to noise ration of the device.

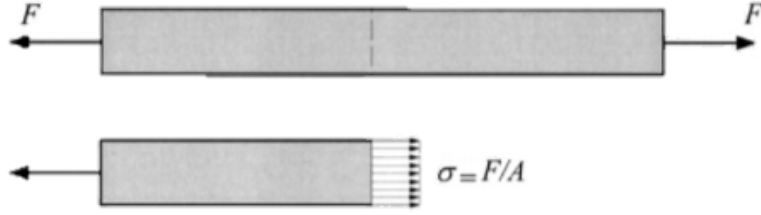


Figure 2: illustration of stress parallel to the normal of the surface [14]

3 Theory

In order to study the wave propagation, the forces that cause waves to propagate through a medium have to be understood. Forces on the liquid salt cause stress and strain, the relation of the stress and strain are expressed using moduli of elasticity like the Young's modulus and Poisson's ratio. First stress and strain will be elaborated and from the definitions of stress and strain the moduli of elasticity will be explained. Finally some different wave types will be explained. These wave types are displacements in specific directions and the behaviour of a specific wave type is dependent on the moduli of elasticity.

3.1 Stress

Stress is the force per area that works on a surface, the force working on the area can be split into component that can be parallel or orthogonal to the normal of the surface as can be seen in figures 2, 3. The stress orthogonal to the normal of the surface is referred to as the shear stress.

When dealing with three dimensional space the stress can be written as a matrix of 3x3 with τ values of shear stress and σ values of normal stress, such a matrix can be seen in equation 1 below [15].

$$\bar{\bar{T}} = \begin{bmatrix} \sigma_{xx} & \tau_{xy} & \tau_{xz} \\ \tau_{yx} & \sigma_{yy} & \tau_{yz} \\ \tau_{zx} & \tau_{zy} & \sigma_{zz} \end{bmatrix} \quad (1)$$

3.2 Strain

Strain is the relative extension of an object, strain is given by equation 2 [14]. Where ϵ is the strain, ΔL the elongation and L_0 the original length.

$$\epsilon = \frac{\Delta L}{L_0} = \frac{\textit{elongation}}{\textit{original length}} \quad (2)$$

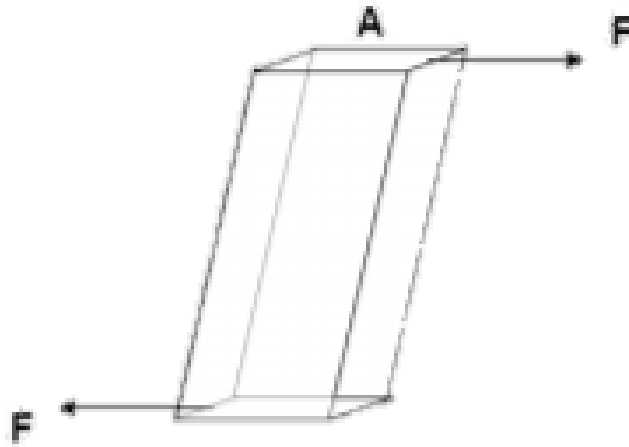


Figure 3: Illustration of stress orthogonal to the normal of the surface [15]

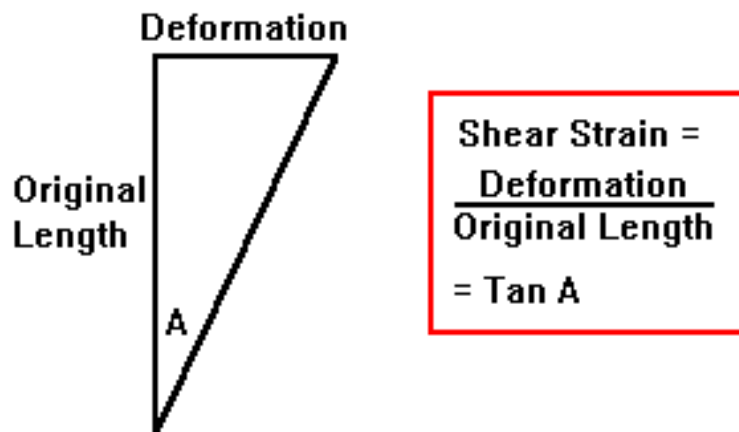


Figure 4: Illustration of shear strain [16]

Like shear stress there is also shear strain this is the deformation perpendicular to the original length as can be seen in figure 4. The normal and shear strains can be combined into a matrix as can be seen below in equation 3. In the figure below normal strains are indicated with ϵ and shear strains with γ , the subscripts indicate the elongation and original length direction.

$$\bar{\bar{T}} = \begin{bmatrix} \epsilon_{xx} & \gamma_{xy} & \gamma_{xz} \\ \gamma_{yx} & \epsilon_{yy} & \gamma_{yz} \\ \gamma_{zx} & \gamma_{zy} & \epsilon_{zz} \end{bmatrix} \quad (3)$$

3.3 Moduli of elasticity

3.3.1 Young's modulus

When a wave travels through a medium it causes deformation and stress on the material. The Young's modulus is a material property that gives the relation between the stress and the strain of the object, with the stress and strain aligned. This relation varies with the temperature of the object and with impurities in the material. The impurities will also effect the temperature dependence of the Young's modulus with temperature. The Young's modulus gives the relation of normal stress and strain through Hooks law equation 4 [17].

$$\sigma = E\epsilon \quad (4)$$

Where σ is the stress in N/m^2 , E the Young's modulus in N/m^2 and ϵ the dimensionless strain.

3.3.2 Shear modulus

Similar to the Young's modulus there is also a shear modulus G given by equation 5 [14].

$$G = \frac{\tau}{\gamma} \quad (5)$$

Where G is the shear modulus in N/m^2 , τ_{xy} is the shear stresses in N/m^2 and γ_{xy} the shear strain which is dimensionless. Like the Young's modulus the shear modulus is also temperature dependant.

3.3.3 Bulk modulus

The Bulk modulus is used to express how resistant an object is to compression, the expression for the Bulk modulus is given by equation 6 [18].

$$K = \frac{\sigma}{\Delta V/V_0} \quad (6)$$

Where K is the Bulk modulus in N/m^2 , ΔV the change of volume in m^3 , V_0 the original volume in m^3 and σ the normal stress in N/m^2 [19]. If the material is elastic isotropic then the Bulk modulus can be expressed in terms of the Young and shear modulus, in fact with any two modulus of elasticity all the others can be defined. Moduli of elasticity being the Young's modulus, the shear modulus, the Bulk modulus which we have discussed as well as the Poisson's ratio, Kirchhoff's modulus and Lamé's constants.

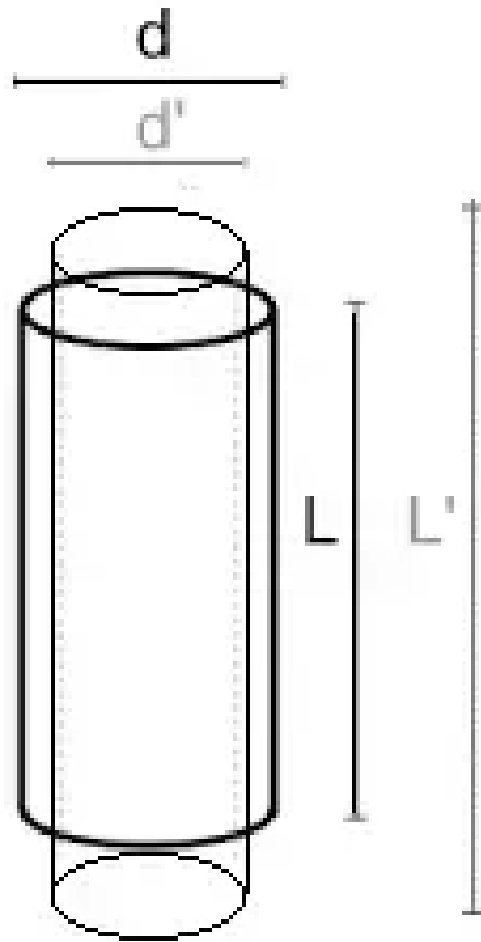


Figure 5: Illustration of the deformation caused by deformation in the orthogonal direction [20]

3.3.4 Poisson's ratio

The Poisson factor or Poisson's ratio gives strain orthogonal to the direction of a known strain an illustration can be seen in figure 5. The Poisson's ratio is given by equation 7[21].

$$\nu_{XY} = -\frac{\epsilon_{XX}}{\epsilon_{YY}} \quad (7)$$

Where ν is the Poisson's ratio [22] which is dimensionless and ϵ_{XX} and ϵ_{YY} the strain in the X and Y direction respectively both of these strains are dimensionless.

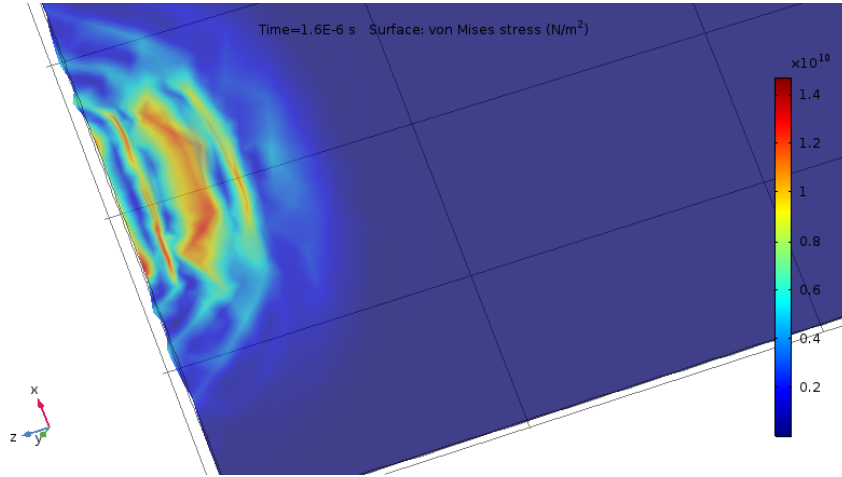


Figure 6: Illustration of a symmetrical lamb wave induced on a plate, the color indicates the surface tension.

3.4 Wave types

Since this experiment is confined to waves in a plate the most important wave types are:

- Lamb waves symmetrical
- Lamb waves asymmetrical
- Shear waves

[15]

3.4.1 Lamb waves symmetrical

Symmetrical lamb waves are longitudinal wave where the direction of propagation is parallel to the displacement that the wave induces. The wave equation for symmetrical lamb waves is given by equation 8 [23].

$$\frac{\delta^2 \zeta}{\delta z^2} = \frac{Y}{\rho} \frac{\delta^2 \zeta}{\delta t^2} \quad (8)$$

In equation 8 ζ is the wave induced displacement along the z axis, Y is the Young's modulus of the medium and ρ is the density of the medium. Symmetrical Lamb waves in a plate are illustrated in figure 6. In 6 a wave was induced at the left edge of the plate along a width less then the width of the plate.

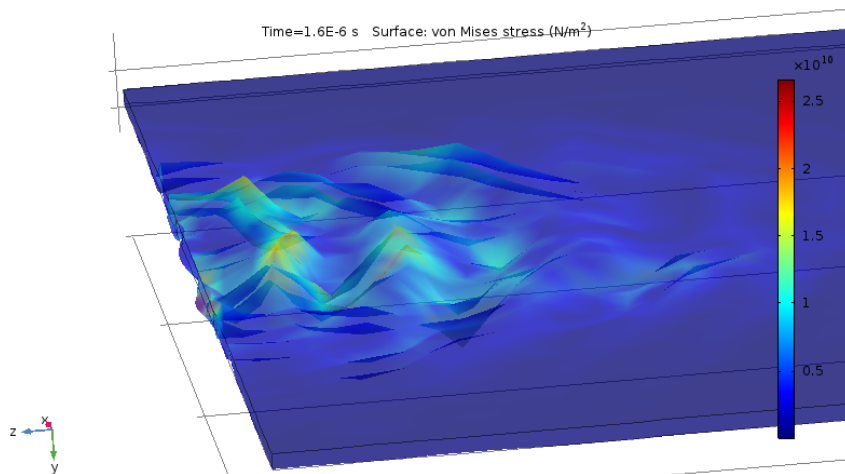


Figure 7: Illustration of a asymmetrical lamb wave induced on a plate, the color indicates the surface tension.

3.4.2 Lamb waves asymmetrical

Asymmetrical Lamb waves are also know as flexural waves, these waves have a direction of propagation orthogonal to the displacement. The displacement of asymmetrical lamb waves is along the normal of the plate. An image of asymmetrical lamb waves on a plate can be seen in figure 7.

3.4.3 Shear waves

Shear waves, also know as in plane wave, have a displacement orthogonal to the displacement of the wave. both the displacement and the propagation direction are orthogonal to the normal of the plate, explaining the name in plane wave. Figure 8 shows shear waves in a plate.

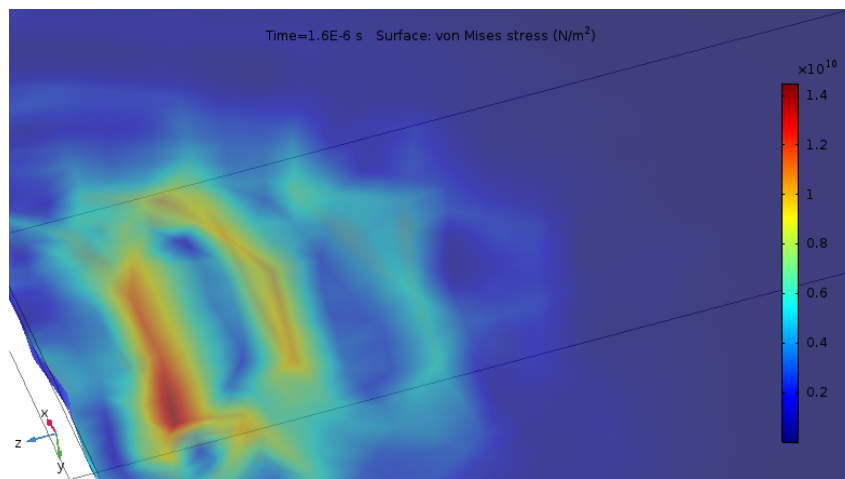


Figure 8: Illustration of shear waves induced on a plate, the color indicates the surface tension.

4 Model

The model has the goal of describing the wave propagation through a nickel plate. The factors that are investigated are the location of the transducer where the wave originates, the polarization of the induced wave and the temperature of the plate. The temperature is varied because during the start up of the reactor the temperature of the molten salt will increase and the effect of these varying temperatures on the wave propagation is important to know in order to be able to perform measurements at all these different temperatures. The wave polarization and the location where the waves are induced can be chosen when designing a measurement device. Differences in these factors can influence the attenuation of the wave and thus change the signal to noise ratio of the device. Knowing the best combination of transducer location and wave polarization is important to know in order to optimize the design.

4.1 simulation

For this experiment the nickel plate is simulated using COMSOL Multiphysics® [1]. Simulations are made for different temperatures and different transducers locations, from these simulations the displacement along each axis as well as the total displacement can be found for each time step. The temperature is changed from 300 to 1000 kelvin in nine equal steps and the transducer is displaced from the center to the edge of the plate in seven equal steps. For the simulations the dimensions for the plate are 20 mm by 0.1 mm by 40 mm in what is referred to as x,y and z direction respectively. The transducer surface where the wave originates is 5 mm by 0.1 mm with the normal of this surface along the z-axis, a representation of the plate with the transducer can be seen in figure 9.

Most of the material properties of nickel are taken from the materials library present in COMSOL Multiphysics® [1]. The thermal expansion coefficient for temperatures above 800 degrees Kelvin are from [24] and the wave velocity for longitudinal, shear and flexural wave at room temperature were taken from [25]. These known wave velocity's are used to determine the size of the mesh elements and time steps used in the simulation.

The wave is induced to the plate by giving a prescribed displacement to the transducer, the prescribed displacement can be seen in equation 9. With f the displacement in a selected direction in *meters*, t the time is *seconds* and A , b , c and d parameters to define the displacement.

$$f(t) = A \cdot \cos(b \cdot t) \cdot e^{-(c(t-d))^2} \quad (9)$$

4.1.1 Discretization

For the discretization of the time a maximum step size of one fifth of the frequency is advised by literature [26]. This is also the step size that is used in this experiment.

For the discretization of space a mesh is generated over the entire geometry, the mesh used can be seen in the figure 10. For the mesh the maximum element size is set to one eighth of the wavelength as advised by literature [26]. Near the edges the mesh becomes finer, than the literature advises so that preciser simulation of wave reflection at the edge of the plate can be obtained. The amount of elements at the edge of the plate is set to make the mesh elements 1.5 times smaller, the smaller mesh elements at the edge improve the simulation of the wave behaviour at the edge of the plate.

4.2 Data processing

By plotting the displacement of the transducer side of the plate and the side opposite of the transducer as a function of time. The wave propagation can be visualizes as can be seen in figure 11. In this figure it can be seen that the transducer causes a displacement at the transducer side of the plate and this causes a wave through the plate that some time later moves the opposite side of the plate.

In order to analyze the displacement of the plate as a function of time an indication for the wave front amplitude and time had to be found. Such an indication can be found by plotting Gaussian curve along the top of the absolute value of these displacement plots and with a Gaussian curve of the form in equation 10 the parameters a, b and c define the curve. a gives and indication for the amplitude of the wave front and b indicates the time corresponding to the maximum displacement. taking the ration between the values of a found from the fitted curve for the transducer and opposite side gives the relative amplitude which indicates the attenuation. subtracting the values of b found from the fitted curve for the transducer and opposite side gives the traveling time of the wave through the length of plate. In equation 10 a, b and c are fit parameters, t is the time in seconds and f is the displacement in meters.

$$f(t) = a * \exp(-((t - b)/c)^2) \quad (10)$$

Figure 12 shows the Gaussian curves fitted of the displacement of the transducer side of the plate, the points used for the Gaussian fit are also shown.

The change in width of the wave pulse can be found by dividing the values of c for the opposite side of the plate by the value of c from the transducer side of the plate. The travel time of the wave from the transducer side to the opposite side is found by taking the difference in value of b between the transducer and opposite side. With this method for determining the wave travel time the dispersion of the wave can have an effect on the travel time because the dispersion will cause the Gaussian curve to shift and increase the wave travel time. A different value for the wave travel time would be found when the first incline curve would be used instead of the top of the Gaussian curve. From the travel time the wave velocity can be calculated since the length of the plate is known.

The relative amplitude of the wave is found by comparing the maximum displacement of the transducer side of the plate and the opposite side of the plate. The relative am-

plitude indicates the attenuation that the wave experiences when traveling through the plate. The attenuation in terms of total energy can be found by taking the ratio between the area underneath the Gaussian curves of the transducer side and the opposite side. The area underneath the curve is proportional to the product of fit parameters a and c , the area underneath a Gaussian curve is given by equation 11.

$$A = a \cdot c\sqrt{2\pi} \quad (11)$$

In equation 11 The area underneath the Gaussian curve is A , a and c are the fit parameters of the Gaussian curve as given from equation 10.

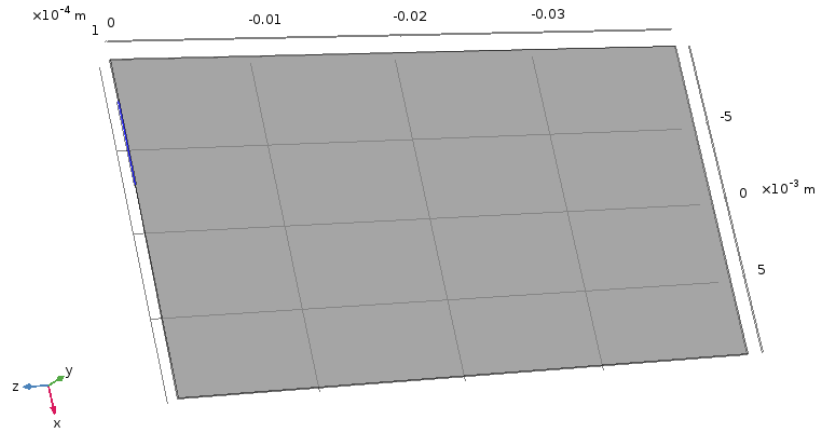


Figure 9: Image of the plate with the transducer in blue, there is no axis along the y axis because the plate thinner than it is wide and long, the axis are denoted in the bottom right corner

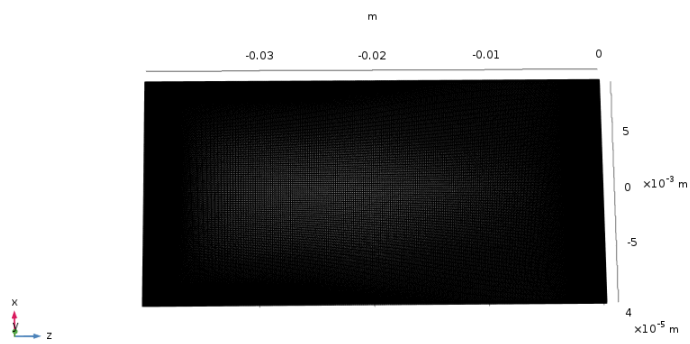


Figure 10: Image of the generated mesh

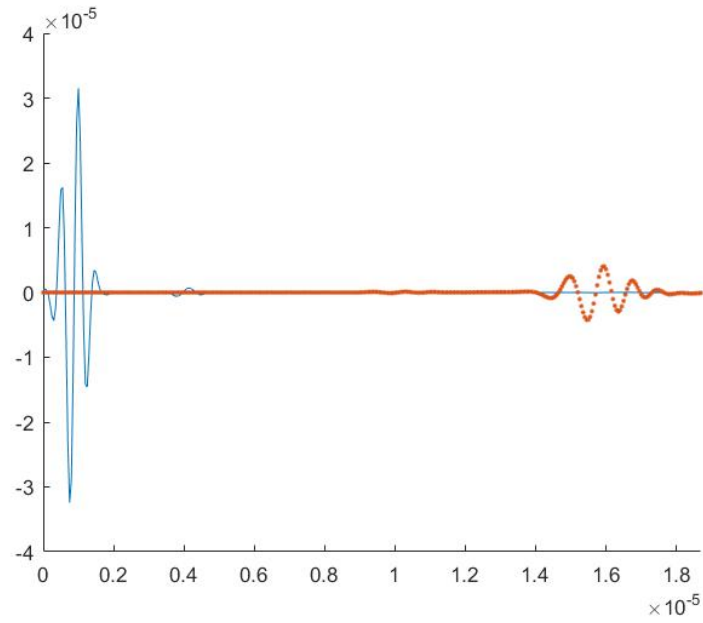


Figure 11: Plot of the displacement along a specific axis for the transducer side and the opposite side represented by the blue line and red dots respectively.

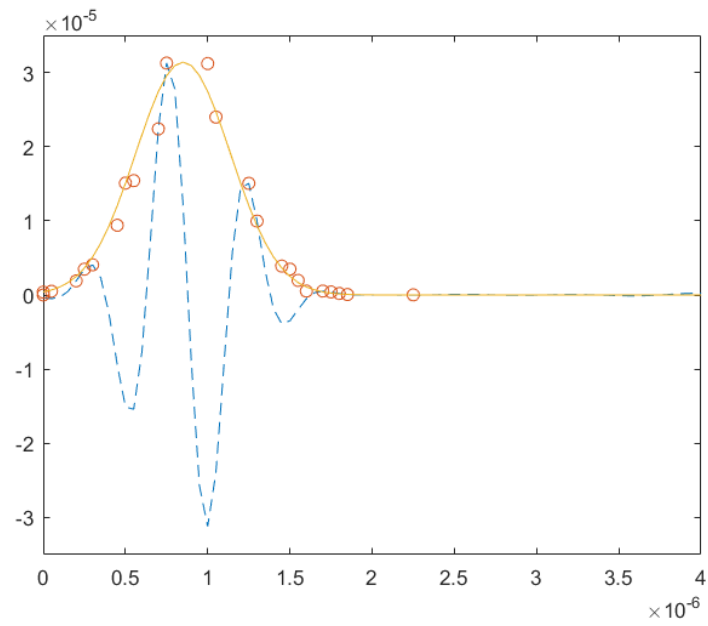


Figure 12: Plot of the displacement with Gaussian curve fitted over the top and the point used to make the fit denoted in the plot with a dashed line a line and circles respectively.

5 Results and Discussion

The effects of temperature, transducer location and wave polarization on the relative amplitude and wave velocity are visualized in figure 16a, 16e, 17, 14, 18 and 15. The travel time plotted in the figures is found by comparing the values of fit parameter b from the Gaussian fit as discussed before in section 4 and from the travel time the wave velocity can easily be found since the length of the plate is known. The travel time is plotted as a function of transducer position and temperature in a surface plot. The relative amplitude is the ratio between the Gaussian wave amplitude (fit parameter a) at either side of the plate. The relative amplitude like the wave travel time is shown as a function of temperature and transducer position in a surface plot, multiple of these surface plots are made for the different wave polarization.

5.1 temperature

From figure 16a, 17 and 18 the effect of temperature on the relative amplitude can be found, by looking at the changes along the temperature axis. It can be seen that for both x and y polarized waves there are certain temperatures that yield higher relative amplitudes when compared to other temperatures, but there is no general trend to one end of the temperature range yielding higher relative amplitudes. The effect of the temperature is at most 0.02. For y polarized waves the absolute effect of temperature on the relative amplitude is of similar scale to the effect on the x polarized waves, however the relative amplitude of y polarized waves is approximately a third that of the x polarized waves causing the temperature to have a relatively larger effect for y polarized waves. For z polarized waves the increase in temperature causes a decrease in relative amplitude with a total decrease around 0.02 as the temperature increases from $300K$ up to $1000K$

From figure 16e, 14 and 15 the effect of temperature on the wave travel time can be found, by looking at the variations in wave travel time along the temperature axis. On average the wave travel time increases with increasing temperatures, except for a clear exception where the wave travel time for wave induced in the y direction sharply increases when the temperature drops from $387.5K$ to $300K$. for y polarized wave the wave travel time varies between 18 and 20 μs for temperatures increasing from $387.5K$ up to $1000K$ giving wave velocities varying from $2.0km/s$ to $2.2km/s$. At $300K$ the wave travel time jump to around $24\mu s$ corresponding to a wave velocity of $1.7km/s$ this value of the wave velocity at $300K$ is lower than the value expected from the theory [25]. There is a clear deviation of the y polarized wave velocity from both the theory at $300K$ and the trend of x and z polarized waves where the wave velocity increases for higher temperatures, this could have been caused by an error made in either the simulation or the data processing. Another option is that there is some physical phenomena that causes these notable results. As said before for both the x and z polarized waves the velocity increases with decreasing temperatures. For z polarized waves the wave travel time increases from $9.0\mu s$ to $10.2\mu s$

with a temperature increases from $300K$ to $1000K$, this corresponds to a wave velocity decrease from $4.5km/s$ to $3.9km/s$. For x polarized waves the wave travel time increases from $14.5\mu s$ to $16.5\mu s$ with a temperature increases from $300K$ to $1000K$, this corresponds to a wave velocity decrease from $2.8km/s$ to $2.5km/s$. The values found for the wave velocity of z and x polarized waves are near the values found in the theory [25], there is still a small deviation that can be attributed to either a small error caused by the simulation or data processing another possibility is that the dimensions of the wave guide have an effect on the wave velocity.

5.2 transducer location

Both x and z polarized waves have relative amplitudes that decrease for larger transducer displacement as can be seen in figure 16a and 18. For x polarized waves the relative amplitude decreases from 0.11 down to 0.04 with the increase in transducer offset away from the centre of the plate. For z polarized waves the relative amplitude is higher and decreases from around 0.16 down to 0.09 with the transducer offset increasing away from the center up to to the very edge of the plate. For y polarized waves it can be seen that there are certain transducer positions that result in a higher relative amplitude see figure 17. For both a transducer offset of $2.5mm$ and a transducer offset of $6.25mm$ the relative amplitude has some significantly higher values with relative amplitudes up to 0.029 between these transducer positions the relative amplitude is lower and when the transducer is centered the relative amplitude is at a minimum around 0.022. the minimum of relative amplitude for a centered transducer is in sharp contrast to the clear increase in relative amplitude for both x and z polarized waves as the transducer is moved towards the centre. An explanation could be that this is an error in the simulation caused by to few mesh elements along the y axis. Another explanation could be that since the sides of the plates are not fixed the wave might experience less attenuation along these edges compared to the centre where there is plate material at either side, this would however not explain the increase in relative amplitude at an offset of $2.5mm$ from the centre. From figure 16e, 14 and 15 the effect of transducer offset on the wave travel time can be found, by looking at the variations in wave travel time along the transducer offset axis. The offset of the area where the waves are induced seems of little impact on the wave travel time when compared to the effect of the plate temperature. for y and z polarized waves no clear correlation between the offset and the wave travel time can be found from the figures. for y and z polarized waves the transducer causes some variation around $0.5\mu s$ with no clear trend. For x polarized waves there seems to be clear decrease in wave travel time as the transducer moves away from the centre. The decrease is around $0.3\mu s$ as the transducer moves from the center to the edge of the plate.

5.3 wave polarization

The relative amplitude for waves induced with x polarization can be seen in figure 16a this can be compared to waves induced and measured in the y and z direction seen in figure 17 and 18 by comparing the surface plots the effect of the wave polarization on the relative amplitude can be found. The x and z polarized waves behave similarly to changes in temperature and transducer position causing the surface plots to look alike. There are differences in the height of the relative amplitude between x, y and z polarized waves. With z polarized waves having a relative amplitude between 0.08 and 0.15, x polarized waves having a relative amplitude between 0.03 and 0.11 and y polarized waves having the lowest relative amplitude between the 0.02 and 0.03. The relative amplitude of y polarized waves does not react similarly to temperature and transducer position when compared to the x and z polarized waves.

From comparing the wave travel time shown in figure 16e, 14 and 15 it can be found that the waves induced in the z direction have the highest wave velocity, when compared to x and y polarized waves. with z polarized waves having a travel time between $9.0\mu s$ and $10.2\mu s$, which corresponds to a wave velocity between $3.9km/s$ and $4.5km/s$. x Polarized waves are slower than z polarized waves but faster than y polarized waves with the wave travel time lying between the $14.5\mu s$ and $16.5\mu s$, which leads to a wave velocity between the $2.8km/s$ and the $2.5km/s$. Waves polarized in the y direction have wave travel times from $18\mu s$ to $24\mu s$ corresponding to wave velocities between the $1.7km/s$ and the $2.2km/s$

5.4 Displacement measurement

Plots similar to the wave travel time can be made for the the attenuation in terms of relative amplitude and relative area under the Gaussian curve. The plots can have significant differences when either the total displacement or only the displacement of the polarization direction is measured. In the figure 16 the relative amplitude, wave travel time and area under the curve is shown in surface plots for the displacement in the polarization direction as well as for the total displacement. The total displacement is found by taking the root of sum of the square of each of the three different polarization directions. The used equation can be seen in equation 12 where d_{total} is the total displacement and d_x , d_y and d_z are the displacements in the x, y and z direction respectively.

$$d_{total} = \sqrt{(d_x)^2 + (d_y)^2 + (d_z)^2} \quad (12)$$

Analyzing the differences between measuring the displacement in the polarization direction of the induced wave or measuring the total displacement, we find that measuring only the polarization direction gives less rigid results 16. This is caused by waves with polarization other than the induced polarization, these waves can be induced by waves with a different polarization traveling through the medium [27]. Waves with different

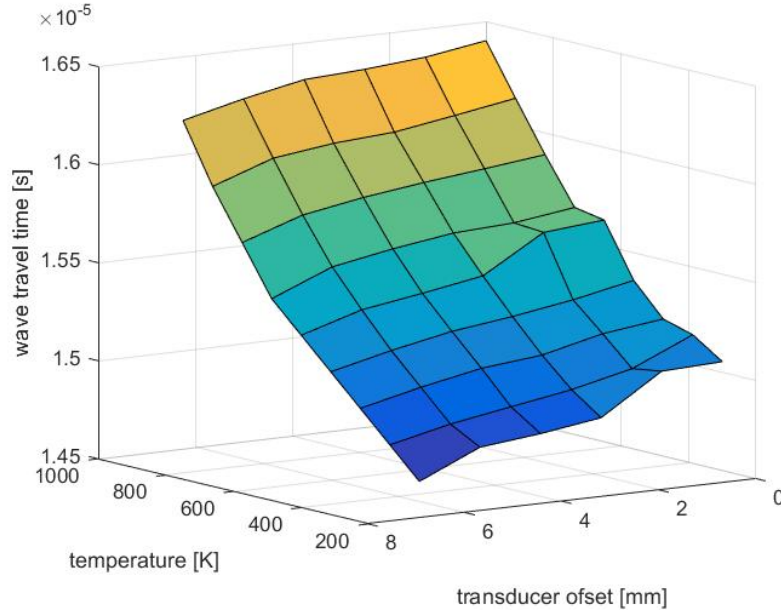


Figure 13: Surface plot of the wave travel time as a function of the transducer offset and temperature with the transducer wave polarized in the x direction, measuring the displacement in the x direction.

polarization can have different velocities and this can cause these waves to arrive at the end of the plate just before or just after the main wave front with polarization in the induced polarization direction. The presence of the wave with different polarization could in the data processing sometimes be considered as part of the wave packet and other times not depending on how much time difference there is between the arrival time of the different waves. the waves with polarization other than the induced polarization sometimes being considered as part of the wave packet and sometimes not could cause the rigidity in the results, since the Gaussian curve could for example shift to a higher travel time when waves that arrived after the main wave packet are considered part of the main wave packet.

Another difference seen between measuring the displacement, in the polarization direction of the induced wave or measuring the total displacement is that measuring the total displacement gives higher relative amplitude and relative wave packet energy. This is because the waves of all different polarization directions are added together in order to obtain the total displacement so this value will never be smaller than the displacement in one direction as can be seen in figure 16. This stronger signal might be usable to obtain better results, however there are also more unwanted signals. Additional signals are received by taking the total displacement instead of only taking the displacement in the polarization direction of the induced wave, these signals can hinder the data processing

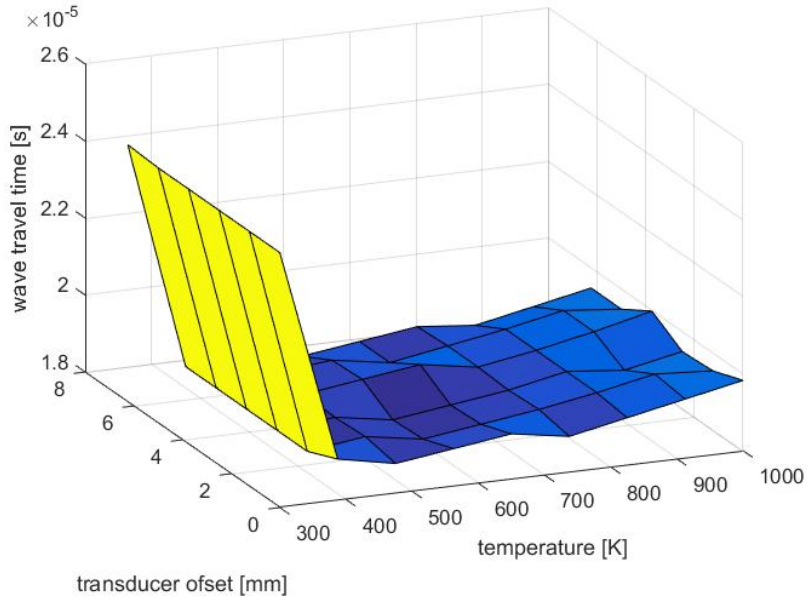


Figure 14: Surface plot of the wave travel time as a function of the transducer offset and temperature with the transducer wave polarized in the y direction, measuring the displacement in the y direction.

and for that reason only the displacement along the polarization of the induced wave is used in this research.

5.5 Uncertainty

One step of the data processing is the fitting of a Gaussian curve, the uncertainty of the found fit parameters can easily be found using the data points used for the fit. The uncertainty up to the point of this fit can be quantified by analyzing the data from the induced wave at the surface where the wave is induced. Because the wave is induced at this surface we know what the correct result should be. By comparing the known correct results to the results acquired through the data processing we can find the deviation that the method has introduced compared to correct results. From the error found by analyzing the surface where the wave is induced it can be deduced that the error in this part of the data processing is smaller than one tenth of the uncertainty caused by the fit, this means that the error can be neglected compared to the uncertainty of the fit. For the rest of the data processing the uncertainty of the fit is used in order to find the standard deviation of the end results.

In order to show the standard deviation of the amplitude attenuation a plot is made for one specific transducer offset, this allows a two dimensional plot of the attenuation

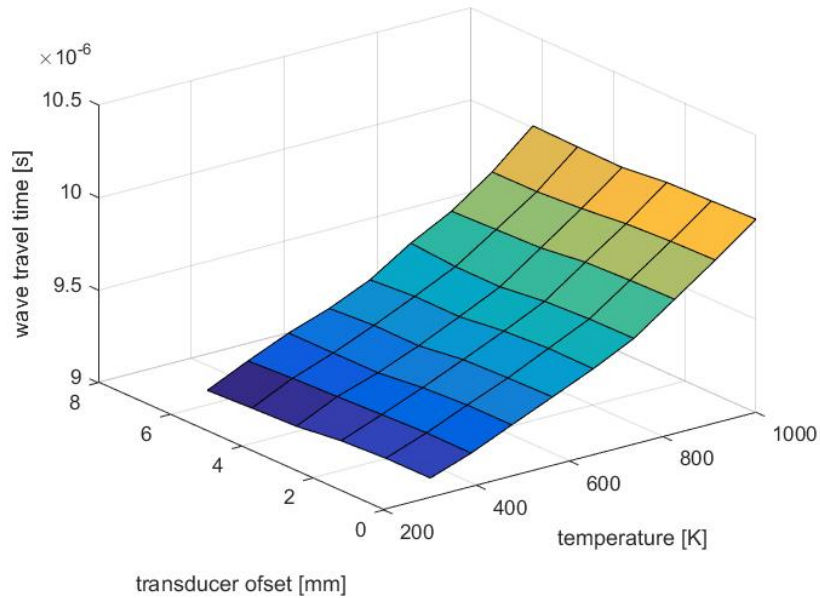
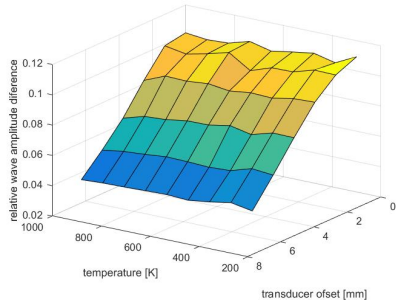
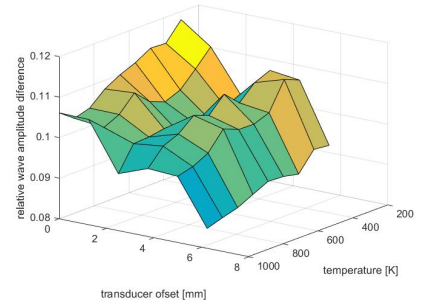


Figure 15: Surface plot of the wave travel time as a function of the transducer offset and temperature with the transducer wave polarized in the z direction, measuring the displacement in the z direction.

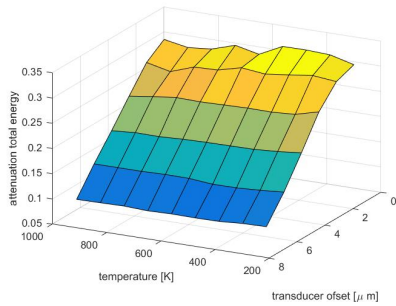
including error bars to indicate the standard deviation this can be seen in figure 19. Like for the amplitude attenuation a similar plot is made for the wave velocity as can be seen in figure 20. The standard deviation of the data is similar for all data points with x or z polarized induced wave, for the y polarized induced waves the standard deviation for the wave velocity is significantly higher. The complete data collection including standard deviations can be found in appendix B.



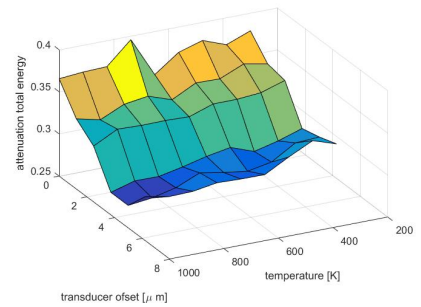
(a) surface plot of the relative amplitude in the x direction for a wave induced with x polarization



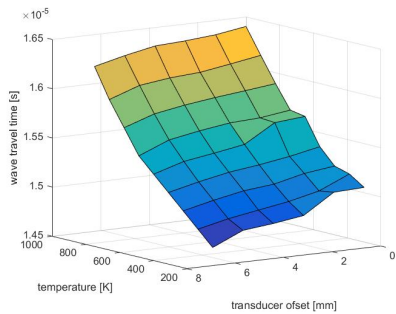
(b) surface plot of the relative amplitude in any direction for a wave induced with x polarization



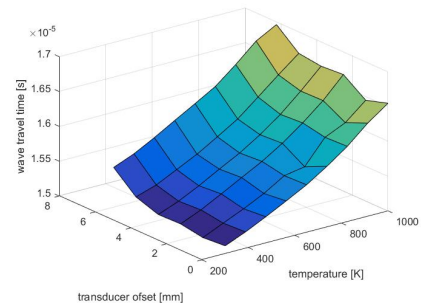
(c) surface plot of the relative wave packet energy measuring displacement in the x for a wave induced with x polarization



(d) surface plot of the relative wave packet energy measuring displacement in any direction for a wave induced with x polarization



(e) surface plot of the wave travel time measuring displacement in the x direction for a wave induced with x polarization



(f) surface plot of the wave travel time measuring displacement in any direction for a wave induced with x polarization

Figure 16: surface plot comparing measuring total displacement with measuring displacement only in the direction of polarization of the induced wave

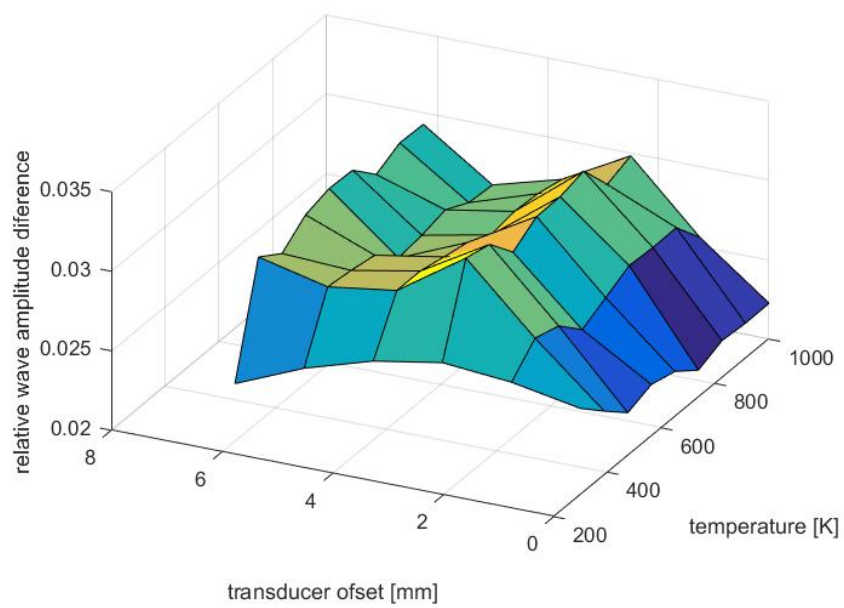


Figure 17: Surface plot of the relative amplitude as a function of the transducer offset and temperature with the transducer wave polarized in the y direction, measuring the displacement in the y direction.

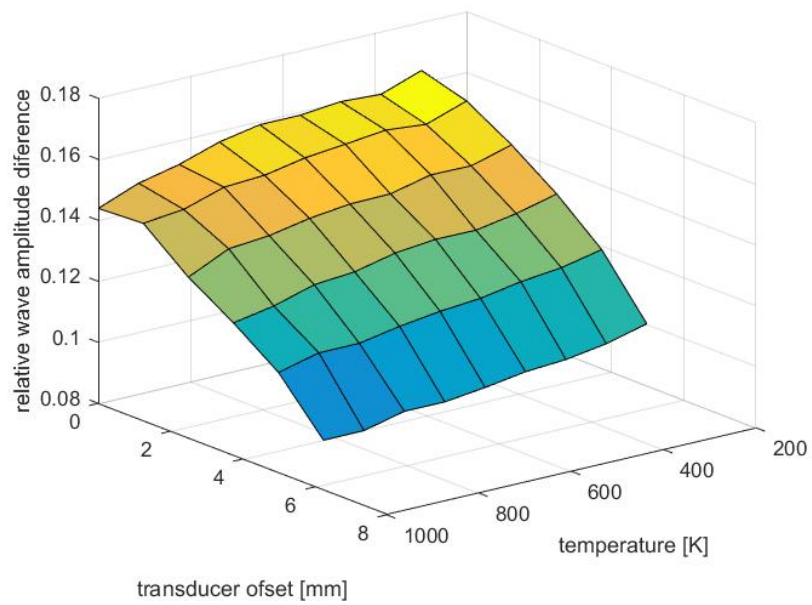


Figure 18: Surface plot of the relative amplitude as a function of the transducer offset and temperature with the transducer wave polarized in the z direction, measuring the displacement in the z direction.

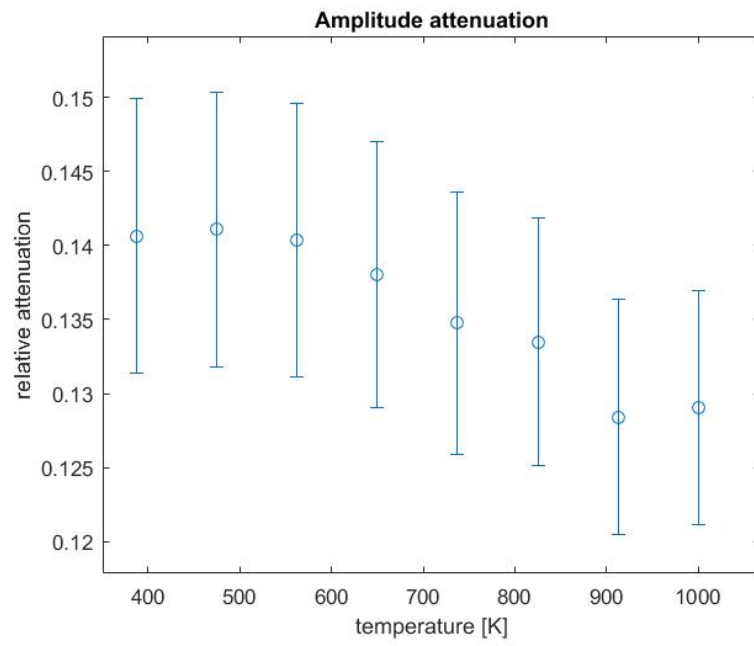


Figure 19: Plot of the amplitude attenuation as a function of temperature with the transducer wave polarized in the z direction and error bars indicate the standard deviation of the data points.

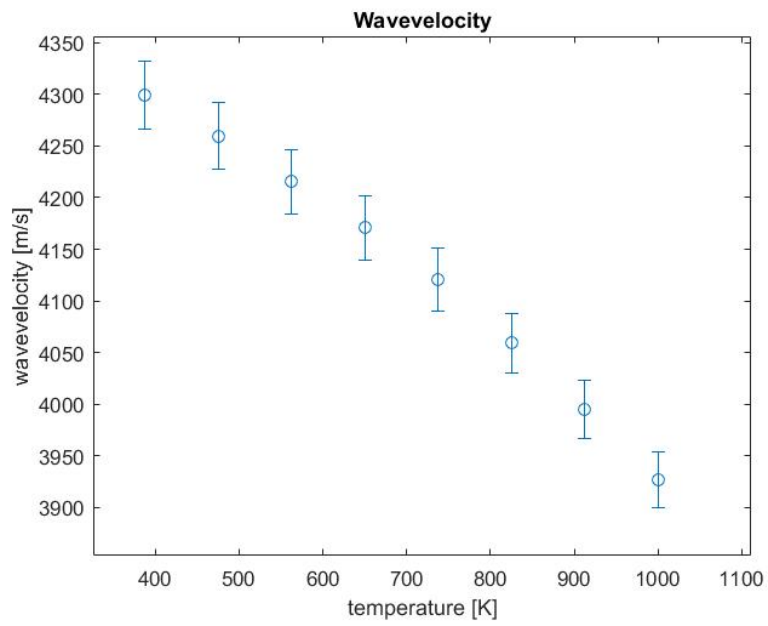


Figure 20: Plot of the wave velocity as a function of temperature with the transducer wave polarized in the z direction and error bars indication the standard deviation of the data points

6 Conclusion

The relative amplitude for waves induced with the polarization parallel to the propagation direction of the wave is higher than the relative amplitude for the waves with the propagation direction orthogonal to the polarization. The waves induced with the polarization parallel to the propagation direction have a relative amplitude of around 0.12 depending on the temperature and transducer position. This means that a stronger signal will pass through the wave-guide compared to using waves with the propagation direction orthogonal to the polarization where the relative amplitudes lies around 0.03 and 0.08 for the y and x directed polarized waves respectively. Beside the highest relative amplitude the waves polarized in the z direction also have the highest wave velocity around 4.0km/s compared to 2.0km/s and 2.6km/s for the y and x polarized waves respectively. The wave velocity decreases at the temperature increases for both the z and x polarized waves. The y polarized waves have the lowest wave velocity also the wave velocity decreases for higher temperatures except for a sharp increases when the temperature drops from 387.5K to 300K . the transducer offset has little effect on the wave velocity compared to the temperature changes. The standard deviation for the relative amplitude lies around 10^{-2} and for the wave velocity around 50m/s varying with temperature, transducer position and wave polarization.

For further research the uncertainty of the results can likely be decreased by using finer time steps and mesh elements in the Comsol simulation [1]. Simulating more different temperatures and transducer positions could give better insight into the temperature and transducer positions influence on the wave propagation, multiple surfaces where waves can be induced simultaneously could also give results helpful for instruments using the ultrasonic waves to perform measurements. In order to work towards an instrument capable of measuring molten salt material properties, the results of this research could be combined with research into the propagation of the waves through the molten salt and the possibilities that there are to measure and induce waves with specific polarization.

References

- [1] Comsol multiphysics® v. 5.3. there is no affiliation with COMSOL AB, COMSOL AB has not authorized, sponsored or approved.
- [2] Ed Nijpels. klimaataakkoord. Technical report, Klimaatberaad, 2018.
- [3] World Nuclear Association. Sustainable energy. Technical report, world nuclear association, 2013.
- [4] Adam Bernstein, Yi-fang Wang, Giorgio Gratta, and Todd West. Nuclear reactor safeguards and monitoring with antineutrino detectors. *Journal of Applied Physics*, 91(7):4672–4676, 2002.
- [5] Gisela Grosch. Gif membership. Technical report, GIF Policy Group, 2017.
- [6] Elisa CAPELLI. *Thermodynamic characterization of salt components for molten salt reactor fuel*. PhD thesis, Delft University of Technology, 2015.
- [7] Thomas J. Dolan. 1 - introduction. In Thomas J. Dolan, editor, *Molten Salt Reactors and Thorium Energy*, pages 1 – 12. Woodhead Publishing, 2017.
- [8] L Mathieu, D Heuer, R Brissot, C Garzenne, C Le Brun, D Lecarpentier, E Liatard, J-M Loiseaux, O Meplan, E Merle-Lucotte, et al. The thorium molten salt reactor: Moving on from the msbr. *Progress in Nuclear Energy*, 48(7):664–679, 2006.
- [9] Jeff Gardiner. Nuclear reactor refueling. Technical report, XCEED, 2018.
- [10] Charles W Forsberg, Per F Peterson, H Zhao, et al. An advanced molten salt reactor using high-temperature reactor technology. In *Proceedings of ICAPP*, volume 4, pages 13–17. Citeseer, 2004.
- [11] Jérôme Serp, Michel Allibert, Ondřej Beneš, Sylvie Delpech, Olga Feynberg, Véronique Ghetta, Daniel Heuer, David Holcomb, Victor Ignatiev, Jan Leen Kloosterman, et al. The molten salt reactor (msr) in generation iv: overview and perspectives. *Progress in Nuclear Energy*, 77:308–319, 2014.
- [12] Faiçal Larachi, André Laurent, Noel Midoux, and G Wild. Experimental study of a trickle-bed reactor operating at high pressure: two-phase pressure drop and liquid saturation. *Chemical Engineering Science*, 46(5-6):1233–1246, 1991.
- [13] George J Janz. *Molten salts handbook*. Elsevier, 2013.
- [14] gross D. *Engineering mechanics. 2, Mechanics of materials*, volume 2. Springer Textbook; Springer: Berlin, 2011.

- [15] Marc van den Berg. *High temperature viscosity determination using the Quasi-Scholte wave*. PhD thesis, Delft University of Technology, 2018.
- [16] hafizuddin. Shear rubber deformation. Technical report, wordpress, 2015.
- [17] Coenraad Hartsuijker and JW Welleman. *Engineering Mechanics: Volume 1: Equilibrium*, volume 1. Springer Science & Business Media, 2007.
- [18] Eric J. Mittemeijer. *Fundamentals of Materials Science*. Springer, Berlin, Heidelberg, 2011.
- [19] Jacek Skrzypek and Artur Ganczarski. *Mechanics of anisotropic materials*. Springer, 2015.
- [20] Pavan Tamiri. What is the poisson ratio? *quora*, 2016.
- [21] Marco Falcioni, Mark J Bowick, Emmanuel Guitter, and Gudmar Thorleifsson. The poisson ratio of crystalline surfaces. *EPL (Europhysics Letters)*, 38(1):67, 1997.
- [22] Tom Proulx. *Mechanics of Time-Dependent Materials and Processes in Conventional and Multifunctional Materials, Volume 3: Proceedings of the 2011 Annual Conference on Experimental and Applied Mechanics*, volume 3. Springer Science & Business Media, 2011.
- [23] William Cronk Elmore, William C Elmore, and Mark A Heald. *Physics of waves*. Courier Corporation, 1969.
- [24] T. G. Kollie. Measurement of the thermal-expansion coefficient of nickel from 300 to 1000 k and determination of the power-law constants near the curie temperature. *Phys. Rev. B*, 16:4872–4881, Dec 1977.
- [25] Xactex Corporation. Accoustic properties for metals in solid form. Technical report, Xactex Corporation, 2018.
- [26] HAJ Froeling. *Causes of spurious echoes by ultrasonic wave simulation*. PhD thesis, bsc. thesis, University of Technology Delft, 2017.
- [27] PA Petcher and S Dixon. Mode mixing in shear horizontal ultrasonic guided waves. *Nondestructive Testing and Evaluation*, 32(2):113–132, 2017.

A Appendix A Matlab code

This section contains the matlab code used to import the data to a .m file followed by the code to process the data. data import code.

```
% load('C:\Users\Arjan\Documents\tu delft\jaar 3\BEP\MATLB\T300z.mat')
% load('C:\Users\Arjan\Documents\tu delft\jaar 3\BEP\MATLB\T300x.mat')
% load('C:\Users\Arjan\Documents\tu delft\jaar 3\BEP\MATLB\T300y.mat')
```

```
i=1:701:4200;
u=1;
%
% dw750zT300=slidex(i(u):700+i(u),1:21);
% u=u+1;
% dw750zT344=slidex(i(u):700+i(u),1:21);
% u=u+1;
% dw750zT388=slidex(i(u):700+i(u),1:21);
% u=u+1;
% dw750zT431=slidex(i(u):700+i(u),1:21);
% u=u+1;
% dw750zT475=slidex(i(u):700+i(u),1:21);
% u=u+1;
% dw750zT519=slidex(i(u):700+i(u),1:21);
% u=u+1;
% dw750zT563=slidex(i(u):700+i(u),1:21);
% u=u+1;
% dw750zT606=slidex(i(u):700+i(u),1:21);
% u=u+1;
% dw750zT650=slidex(i(u):700+i(u),1:21);
% u=u+1;
% dw750zT694=slidex(i(u):700+i(u),1:21);
% u=u+1;
% dw750zT738=slidex(i(u):700+i(u),1:21);
% u=u+1;
% dw750zT781=slidex(i(u):700+i(u),1:21);
% u=u+1;
% dw750zT825=slidex(i(u):700+i(u),1:21);
% u=u+1;
% dw750zT869=slidex(i(u):700+i(u),1:21);
% u=u+1;
% dw750zT913=slidex(i(u):700+i(u),1:21);
% u=u+1;
% dw750zT956=slidex(i(u):700+i(u),1:21);
% u=u+1;
% dw750zT1000=slidex(i(u):700+i(u),1:21);
% u=u+1;
% dw750zT1044=slidex(i(u):700+i(u),1:21);
```

```

% u=u+1;

dw0zT300=slidex(i(u):700+i(u),1:21);
u=u+1;
dw125zT300=slidex(i(u):700+i(u),1:21);
u=u+1;
dw250zT300=slidex(i(u):700+i(u),1:21);
u=u+1;
dw375zT300=slidex(i(u):700+i(u),1:21);
u=u+1;
dw500zT300=slidex(i(u):700+i(u),1:21);
u=u+1;
dw625zT300=slidex(i(u):700+i(u),1:21);
u=u+1;
%
% dw0zT431=slidex(i(u):700+i(u),1:21);
% u=u+1;
% dw125zT431=slidex(i(u):700+i(u),1:21);
% u=u+1;
% dw250zT431=slidex(i(u):700+i(u),1:21);
% u=u+1;
% dw375zT431=slidex(i(u):700+i(u),1:21);
% u=u+1;
% dw500zT431=slidex(i(u):700+i(u),1:21);
% u=u+1;
% dw625zT431=slidex(i(u):700+i(u),1:21);
% u=u+1;
%
% dw0zT519=slidex(i(u):700+i(u),1:21);
% u=u+1;
% dw125zT519=slidex(i(u):700+i(u),1:21);
% u=u+1;
% dw250zT519=slidex(i(u):700+i(u),1:21);
% u=u+1;
% dw375zT519=slidex(i(u):700+i(u),1:21);
% u=u+1;
% dw500zT519=slidex(i(u):700+i(u),1:21);
% u=u+1;
% dw625zT519=slidex(i(u):700+i(u),1:21);
% u=u+1;
%
% dw0zT606=slidex(i(u):700+i(u),1:21);
% u=u+1;
% dw125zT606=slidex(i(u):700+i(u),1:21);
% u=u+1;
% dw250zT606=slidex(i(u):700+i(u),1:21);
% u=u+1;
% dw375zT606=slidex(i(u):700+i(u),1:21);

```

```

% u=u+1;
% dw500zT606=slidex(i(u):700+i(u),1:21);
% u=u+1;
% dw625zT606=slidex(i(u):700+i(u),1:21);
% u=u+1;
%
% dw0zT694=slidex(i(u):700+i(u),1:21);
% u=u+1;
% dw125zT694=slidex(i(u):700+i(u),1:21);
% u=u+1;
% dw250zT694=slidex(i(u):700+i(u),1:21);
% u=u+1;
% dw375zT694=slidex(i(u):700+i(u),1:21);
% u=u+1;
% dw500zT694=slidex(i(u):700+i(u),1:21);
% u=u+1;
% dw625zT694=slidex(i(u):700+i(u),1:21);
% u=u+1;
%
% dw0zT781=slidex(i(u):700+i(u),1:21);
% u=u+1;
% dw125zT781=slidex(i(u):700+i(u),1:21);
% u=u+1;
% dw250zT781=slidex(i(u):700+i(u),1:21);
% u=u+1;
% dw375zT781=slidex(i(u):700+i(u),1:21);
% u=u+1;
% dw500zT781=slidex(i(u):700+i(u),1:21);
% u=u+1;
% dw625zT781=slidex(i(u):700+i(u),1:21);
% u=u+1;
%
% dw0zT869=slidex(i(u):700+i(u),1:21);
% u=u+1;
% dw125zT869=slidex(i(u):700+i(u),1:21);
% u=u+1;
% dw250zT869=slidex(i(u):700+i(u),1:21);
% u=u+1;
% dw375zT869=slidex(i(u):700+i(u),1:21);
% u=u+1;
% dw500zT869=slidex(i(u):700+i(u),1:21);
% u=u+1;
% dw625zT869=slidex(i(u):700+i(u),1:21);
% u=u+1;
%
% dw0zT956=slidex(i(u):700+i(u),1:21);
% u=u+1;
% dw125zT956=slidex(i(u):700+i(u),1:21);
% u=u+1;

```

```

% dw250zT956=slidex(i(u):700+i(u),1:21);
% u=u+1;
% dw375zT956=slidex(i(u):700+i(u),1:21);
% u=u+1;
% dw500zT956=slidex(i(u):700+i(u),1:21);
% u=u+1;
% dw625zT956=slidex(i(u):700+i(u),1:21);
% u=u+1;
%
% dw0zT1044=slidex(i(u):700+i(u),1:21);
% u=u+1;
% dw125zT1044=slidex(i(u):700+i(u),1:21);
% u=u+1;
% dw250zT1044=slidex(i(u):700+i(u),1:21);
% u=u+1;
% dw375zT1044=slidex(i(u):700+i(u),1:21);
% u=u+1;
% dw500zT1044=slidex(i(u):700+i(u),1:21);
% u=u+1;
% dw625zT1044=slidex(i(u):700+i(u),1:21);

```

```
clear i u
```

data processing code.

```

clear all
%load('C:\Users\Arjan\Documents\tu delft\jaar 3\BEP\new_data\complete.mat')
load('C:\Users\Arjan\Documents\tu delft\jaar 3\BEP\MATLAB\complete2.mat')

```

```

tic
u=1;
colom=20;          %x=14 y=16 z=18 total=20
offset=6;
tempe=387.5:87.5:1000;
spacee=0:1.25:6.25;
temps=length(tempe);
%y small temperature range
%for y=[dw0yT300,dw0yT388,dw0yT475,dw0yT563,dw0yT650,dw125yT300,dw125yT388,dw125yT475,dw125yT563,dw125yT650]
%complete y
%for y=[dw0yT300,dw0yT388,dw0yT475,dw0yT563,dw0yT650,dw0yT738,dw0yT825,dw0yT913,dw0yT1000]
%y no T=300
for y=[dw0xT388,dw0xT475,dw0xT563,dw0xT650,dw0xT738,dw0xT825,dw0xT913,dw0xT1000,dw125xT388,dw125xT475,dw125xT563,dw125xT650]

```

matrix(:,u)=y;

```

u=u+1;
end

%%
colom=colom*ones(1, size(matrix,2)/21);
p=(u-1)/21;
high=zeros(1,p);

high2=zeros(1,p);

for u=1:p
    clear A B C D max Y Y2 t i j lhi rhi
    Y=matrix(:, colom(u)+21*(u-1));
    Y2=matrix(:, 1+colom(u)+21*(u-1));
    t=matrix(:, 1+21*(u-1));
    % Y=dw375yT650(:,18);
    % Y2=dw375yT650(:,19);
    % t=dw375yT650(:,1);

    j=1;

    for i=1:length(Y')
        if abs(Y(i))>high(u)
            high(u)=abs(Y(i));
            maxim=i;

            end
        end

    b3(u)=t(maxim);

    lhi=0;
    for i=max([2,maxim-50]):maxim
        if abs(Y(i))>abs(Y(i+1)) && abs(Y(i))>abs(Y(i-1))
            lhi=abs(Y(i));
            B(j)=abs(Y(i));
            A(j)=t(i);
            j=j+1;
        end
    end
    end
    j=1;
    rhi=0;
    for i=flip(maxim:min([maxim+100,length(Y')-1]))
        if abs(Y(i))>abs(Y(i+1)) && abs(Y(i))>abs(Y(i-1))
            % if abs(Y(i))>abs(Y(i-1)) && abs(Y(i))>abs(Y(i+1))
            rhi=abs(Y(i));

```

```

        D(j)=abs(Y(i));
        C(j)=abs(t(i));
        j=j+1;
    %     end
    end
end

B=[zeros(1,6),B,flip(D)];
A=[zeros(1,6),A,flip(C)];
X=fit(A.',B.', 'gauss1');
%
% figure
% plot(t,abs(Y),'--')
% hold on
% % axis([0 0.4*10^-5 -3.5*10^-5 3.5*10^-5])
% plot(A,B,'o')
% plot(X)
%
clear A B C D maxim

j=1;

for i=1:length(Y2')
    if abs(Y2(i))>high2(u)
        high2(u)=abs(Y2(i));
        maxim=i;

        end
end
b4(u)=t(maxim);

lhi=0;

for i=max([2,maxim-50]):maxim
% for i=1:max
    if abs(Y2(i))>abs(Y2(i+1)) && abs(Y2(i))>abs(Y2(i-1))
        lhi=abs(Y2(i));
        B(j)=abs(Y2(i));
        A(j)=t(i);
        j=j+1;
    end
end
end
j=1;
rhi=0;
for i=flip(maxim:min([maxim+100,length(Y2')-1]))
% for i=flip(max:length(Y2'))
    if abs(Y2(i))>abs(Y2(i+1)) && abs(Y2(i))>abs(Y2(i-1))
%     if abs(Y(i))>abs(Y(i-1)) && abs(Y(i))>abs(Y(i+1))
        rhi=abs(Y2(i));
    end
end

```

```

        D(j)=abs(Y2(i));
        C(j)=abs(t(i));
        j=j+1;
%         end
    end
end

B=[zeros(1,6),B,flip(D)];
A=[zeros(1,6),A,flip(C)];
X2=fit(A.',B.', 'gauss1');
% f(x) = a1*exp(-(x-b1)/c1)^2
% Coefficients (with 95% confidence bounds):
%     a1 = 4.943e-06 ; %amplitude
%     b1 = 1.208e-05 ; %time of arival
%     c1 = 9.418e-07;
% area under a gaussian curve is a*c*sqrt(2*pi)
%
% plot(t,abs(Y2))
% hold on
% plot(A,B,'x')
% plot(X2)
mar1=confint(X);
mar1a(:,u)=mar1(:,1);
mar1b(:,u)=mar1(:,2);
mar1c(:,u)=mar1(:,3);
x=coeffvalues(X);
a1(u)=x(1);
b1(u)=x(2);
c1(u)=x(3);
x2=coeffvalues(X2);
a2(u)=x2(1);
b2(u)=x2(2);
c2(u)=x2(3);
mar2=confint(X2);
mar2a(:,u)=mar2(:,1);
mar2b(:,u)=mar2(:,2);
mar2c(:,u)=mar2(:,3);

end
marlap=abs(mar1a(1,:)-a1)./1.96;
marlan=abs(mar1a(2,:)-a1)./1.96;
mar2ap=abs(mar2a(1,:)-a2)./1.96;
mar2an=abs(mar2a(2,:)-a2)./1.96;

mar1bp=abs(mar1b(1,:)-b1)./1.96;
mar1bn=abs(mar1b(2,:)-b1)./1.96;
mar2bp=abs(mar2b(1,:)-b2)./1.96;
mar2bn=abs(mar2b(2,:)-b2)./1.96;

```

```

mar1cp=abs(mar1c(1,:)-c1)./1.96;
mar1cn=abs(mar1c(2,:)-c1)./1.96;
mar2cp=abs(mar2c(1,:)-c2)./1.96;
mar2cn=abs(mar2c(2,:)-c2)./1.96;

% errorbar(1:u,a1,mar1an,mar1ap,'vertical')
% hold on
% errorbar(1:u,a2,mar2an,mar2ap,'vertical')

a1=6/(7*sqrt(2*pi))*10^-10*10^6*ones(1,u);
b1=7/8*10^-6*ones(1,u);
c1=7/(12*10^6*sqrt(2))*ones(1,u);
% a1=high;
% a2=high2;

for q1=0:p/temps-1

A1(q1+1,:)=a1(1+q1*temps:temps+q1*temps);
A2(q1+1,:)=a2(1+q1*temps:temps+q1*temps);
eA1p(q1+1,:)=mar1ap(1+q1*temps:temps+q1*temps);
eA1n(q1+1,:)=mar1an(1+q1*temps:temps+q1*temps);
eA2p(q1+1,:)=mar2ap(1+q1*temps:temps+q1*temps);
eA2n(q1+1,:)=mar2an(1+q1*temps:temps+q1*temps);
B1(q1+1,:)=b1(1+q1*temps:temps+q1*temps);
B2(q1+1,:)=b2(1+q1*temps:temps+q1*temps);
eB1p(q1+1,:)=mar1bp(1+q1*temps:temps+q1*temps);
eB1n(q1+1,:)=mar1bn(1+q1*temps:temps+q1*temps);
eB2p(q1+1,:)=mar2bp(1+q1*temps:temps+q1*temps);
eB2n(q1+1,:)=mar2bn(1+q1*temps:temps+q1*temps);
C1(q1+1,:)=c1(1+q1*temps:temps+q1*temps);
C2(q1+1,:)=c2(1+q1*temps:temps+q1*temps);
eC1p(q1+1,:)=mar1cp(1+q1*temps:temps+q1*temps);
eC1n(q1+1,:)=mar1cn(1+q1*temps:temps+q1*temps);
eC2p(q1+1,:)=mar2cp(1+q1*temps:temps+q1*temps);
eC2n(q1+1,:)=mar2cn(1+q1*temps:temps+q1*temps);
% B1=[b1(1:18);b1(19:36);b1(37:54);b1(55:72);b1(73:90);b1(91:108);b1(109:126)];
% B2=[b2(1:18);b2(19:36);b2(37:54);b2(55:72);b2(73:90);b2(91:108);b2(109:126)];
%
% C1=[c1(1:18);c1(19:36);c1(37:54);c1(55:72);c1(73:90);c1(91:108);c1(109:126)];
% C2=[c2(1:18);c2(19:36);c2(37:54);c2(55:72);c2(73:90);c2(91:108);c2(109:126)];

end
v=40*10^-3./(B2(ofset,:)-B1(ofset,:));
eVp=40*10^-3.*(eB2n(ofset,:)).*(B2(ofset,:)-B1(ofset,:)).^-2;
eVn=40*10^-3.*(eB2p(ofset,:)).*(B2(ofset,:)-B1(ofset,:)).^-2;
TEMPE=[tempe,tempe,tempe,tempe,tempe,tempe];
% ampli=(C2(5,:)).*(A2(5,:))./((A1(5,:)).*C1(1,:));

```



```

% ampli=ampli(1)./ampli-1;

ampli=(A2(ofset,:))./(A1(ofset,:));
eAp=(eA2p(ofset,:))./(A1(ofset,:));
eAn=(eA2n(ofset,:))./(A1(ofset,:));
% ampli=ampli(1)./ampli-1;

%c2=amplitude
%c2=time of arival
%c2=
% area under a gaussian curve is a*c*sqrt(2*pi)

figure('name','energy attenuation')

surf(tempe, spacee, (A2.*C2)./(A1.*C1))
xlabel('temperature [K]')
ylabel('transducer ofset [\mu m]')
zlabel('attenuation total energy')
% hold on
% Eerrorp=sqrt(((eA2p.*C2)./(A2.*C1)).^2+((A2.*eC2p)./(A2.*C1)).^2);
% Eerrorn=sqrt(((eA2n.*C2)./(A2.*C1)).^2+((A2.*eC2n)./(A2.*C1)).^2);
% surf([tempe, spacee], (A2.*C2)./(A1.*C1)+Eerrorp, (A2.*C2)./(A1.*C1)-Eerrorn, '_')
figure

surf(tempe, spacee, B2-B1)
xlabel('temperature [K]')
ylabel('transducer ofset [mm]')
zlabel('wave travel time [s]')

figure

surf(tempe, spacee, A2./A1)
xlabel('temperature [K]')
ylabel('transducer ofset [mm]')
zlabel('relative wave amplitude diference')

figure
surf(tempe, spacee, C2./C1)
xlabel('temperature [K]')
ylabel('transducer ofset [mm]')
zlabel('relative width diference')
%%
figure
errorbar(tempe, v, eVn, eVp, zeros(1, length(tempe)), zeros(1, length(tempe)), 'o')
fit=fit(tempe.', v.', 'poly2', 'weights', 1./(eVn.^2+eVp.^2)) ;
hold on
%plot(fit)
xlabel('temperature [K]')
ylabel('wavevelocity [m/s]')

```

```

title('Wavevelocity')
clear fit

figure
errorbar(tempe, ampli, eAn, eAp, zeros(1, length(tempe)), zeros(1, length(tempe)), 'o')

uij=fit(tempe.', ampli.', 'poly2', 'weight', 1./(eAn.^2+eAp.^2));
hold on
% axis([200,1100 -0.05 0.50])

%plot(uij)
xlabel('temperature [K]')
ylabel('relative attenuation')
title('Amplitude attenuation')
toc
xlswrite('yA1.xls', A1)
xlswrite('xA2.xls', A2)
xlswrite('yB1.xls', B1)
xlswrite('xB2.xls', B2)
xlswrite('yC1.xls', C1)
xlswrite('xC2.xls', C2)
xlswrite('yeA1p.xls', eA1p)
xlswrite('xeA2p.xls', abs(eA2p))
xlswrite('yeB1p.xls', eB1p)
xlswrite('xeB2p.xls', abs(eB2p))
xlswrite('yeC1p.xls', eC1p)
xlswrite('xeC2p.xls', abs(eC2p))
xlswrite('yeA1n.xls', eA1n)
xlswrite('yeA2n.xls', eA2n)
xlswrite('yeB1n.xls', eB1n)
xlswrite('yeB2n.xls', eB2n)
xlswrite('yeC1n.xls', eC1n)
xlswrite('yeC2n.xls', eC2n)%, A2n, B1n, B2n, C1n, C2n, eA1nn, eA2nn, eB1nn, eB2nn, eC1nn, eC2nn, eA1n

```

B Appendix B data

Each table displays one data set of fit parameters where the offset is changed along the vertical axis and the temperature is changed along the horizontal axis. the offset range is from 0mm or center up to 6.25mm in steps of 1.25mm and the temperature range is up from 300K to 1000K in steps of 87.5K. The wave polarization and fit parameter corresponding to a data set are listed in the captions.

Table 1: fit parameter A from data from the opposite side from where the wave was induced, with the induced wave polarized in the x direction.

3,88021E-06	3,88764E-06	3,81265E-06	3,75898E-06	3,68673E-06	3,57304E-06	3,53443E-06	3,6289E-06
3,71394E-06	3,58481E-06	3,53236E-06	3,58211E-06	3,7039E-06	3,56967E-06	3,50822E-06	3,62307E-06
3,44682E-06	3,38631E-06	3,40107E-06	3,37015E-06	3,45214E-06	3,42975E-06	3,42177E-06	3,2164E-06
3,70031E-06	3,57692E-06	3,69807E-06	3,56647E-06	3,61419E-06	3,50573E-06	3,45123E-06	3,30949E-06
3,77617E-06	3,54331E-06	3,49483E-06	3,49806E-06	3,55057E-06	3,39486E-06	3,32802E-06	3,2947E-06
3,23666E-06	3,0761E-06	3,10349E-06	3,1106E-06	3,04841E-06	2,98447E-06	2,947E-06	2,90537E-06

Table 2: standard deviation for fit parameter A from data from the opposite side from where the wave was induced, with the induced wave polarized in the x direction.

2,1095E-07	2,09925E-07	2,13641E-07	2,08871E-07	2,03037E-07	1,83348E-07	1,79855E-07	1,89519E-07
2,22805E-07	2,14965E-07	2,02632E-07	2,08973E-07	2,42245E-07	2,18215E-07	2,15564E-07	2,29213E-07
1,98211E-07	1,90412E-07	1,90692E-07	1,89626E-07	1,91979E-07	1,93333E-07	1,86094E-07	1,59946E-07
2,2408E-07	2,10158E-07	2,21689E-07	2,09641E-07	2,20397E-07	2,08906E-07	2,00049E-07	1,94027E-07
2,28655E-07	2,16443E-07	2,1295E-07	2,08757E-07	2,10364E-07	1,97019E-07	1,93526E-07	2,03289E-07
2,64109E-07	2,53462E-07	2,44902E-07	2,50076E-07	2,55626E-07	2,37198E-07	2,32481E-07	2,06321E-07

Table 3: fit parameter B from data from the opposite side from where the wave was induced, with the induced wave polarized in the x direction.

1,61112E-05	1,62525E-05	1,64022E-05	1,65572E-05	1,67451E-05	1,6955E-05	1,72107E-05	1,74195E-05
1,60944E-05	1,62226E-05	1,63664E-05	1,65447E-05	1,65958E-05	1,69417E-05	1,70749E-05	1,73194E-05
1,61415E-05	1,62942E-05	1,64512E-05	1,66063E-05	1,67896E-05	1,70053E-05	1,72491E-05	1,75456E-05
1,61233E-05	1,62676E-05	1,64297E-05	1,6584E-05	1,67696E-05	1,69845E-05	1,72419E-05	1,75223E-05
1,62132E-05	1,63572E-05	1,65008E-05	1,66735E-05	1,68528E-05	1,70904E-05	1,73322E-05	1,75632E-05
1,65176E-05	1,6672E-05	1,68414E-05	1,70064E-05	1,71766E-05	1,74141E-05	1,76738E-05	1,78333E-05

Table 4: standard deviation for fit parameter B from data from the opposite side from where the wave was induced, with the induced wave polarized in the x direction.

7,33094E-08	7,43162E-08	7,70001E-08	7,41745E-08	7,44691E-08	6,45126E-08	6,44047E-08	6,43282E-08
8,10452E-08	8,12789E-08	7,82222E-08	7,46311E-08	7,98388E-08	8,18025E-08	7,69091E-08	7,58266E-08
8,17124E-08	8,08115E-08	8,04864E-08	7,89516E-08	7,74341E-08	7,68629E-08	7,4445E-08	7,03509E-08
6,76744E-08	6,67202E-08	6,84378E-08	6,66403E-08	6,91179E-08	6,7286E-08	6,66652E-08	6,78428E-08
7,10692E-08	7,30139E-08	7,27131E-08	7,07198E-08	7,25078E-08	7,15673E-08	7,2304E-08	7,50678E-08
1,25291E-07	1,15582E-07	1,03126E-07	1,04003E-07	1,17164E-07	1,06197E-07	1,07255E-07	9,09732E-08

Table 5: fit parameter C from data from the opposite side from where the wave was induced, with the induced wave polarized in the x direction.

1,33684E-06	1,37214E-06	1,36732E-06	1,30798E-06	1,51331E-06	1,45653E-06	1,46855E-06	1,42072E-06
1,36863E-06	1,36977E-06	1,39254E-06	1,31604E-06	1,30947E-06	1,34249E-06	1,31379E-06	1,29793E-06
1,39814E-06	1,41336E-06	1,40666E-06	1,37891E-06	1,35015E-06	1,35745E-06	1,36482E-06	1,38772E-06
1,143E-06	1,15478E-06	1,15554E-06	1,17771E-06	1,13468E-06	1,14604E-06	1,16524E-06	1,18025E-06
1,16886E-06	1,17684E-06	1,17144E-06	1,18577E-06	1,18838E-06	1,19229E-06	1,18777E-06	1,1854E-06
1,44247E-06	1,45368E-06	1,37079E-06	1,36855E-06	1,40118E-06	1,40908E-06	1,42313E-06	1,46979E-06

Table 6: standard deviation for fit parameter C from data from the opposite side from where the wave was induced, with the induced wave polarized in the x direction.

9,7123E-08	9,77942E-08	1,04799E-07	1,02801E-07	1,0598E-07	9,26456E-08	9,32653E-08	9,11927E-08
1,12994E-07	1,13376E-07	1,05328E-07	1,01956E-07	1,19221E-07	1,18003E-07	1,09523E-07	1,04323E-07
1,16544E-07	1,16291E-07	1,14604E-07	1,1359E-07	1,09709E-07	1,09753E-07	1,03597E-07	9,82282E-08
9,40356E-08	9,20598E-08	9,30982E-08	9,27021E-08	9,42367E-08	9,09899E-08	9,0096E-08	9,39442E-08
9,62118E-08	9,88833E-08	9,84351E-08	9,68689E-08	9,63191E-08	9,50726E-08	9,58056E-08	9,62157E-08
1,71414E-07	1,62826E-07	1,36147E-07	1,39371E-07	1,63893E-07	1,42667E-07	1,42618E-07	1,27211E-07

Table 7: fit parameter A from data from the opposite side from where the wave was induced, with the induced wave polarized in the y direction.

1,26841E-06	1,33004E-06	1,29111E-06	1,25321E-06	1,29478E-06	1,07852E-06	1,19802E-06	1,22953E-06
1,35064E-06	1,09188E-06	1,21581E-06	1,28937E-06	1,25945E-06	1,22138E-06	1,28441E-06	1,28698E-06
1,25961E-06	1,26363E-06	1,26668E-06	1,24254E-06	1,23511E-06	1,23416E-06	1,21815E-06	1,18917E-06
1,24287E-06	1,18251E-06	1,22966E-06	1,21796E-06	1,23734E-06	1,1696E-06	1,16159E-06	1,20684E-06
1,15778E-06	1,20226E-06	1,20652E-06	1,2026E-06	1,13206E-06	1,15973E-06	1,17829E-06	1,11325E-06
1,19634E-06	1,19672E-06	1,16801E-06	1,15135E-06	1,18907E-06	1,15202E-06	1,11946E-06	1,14772E-06

Table 8: standard deviation for fit parameter A from data from the opposite side from where the wave was induced, with the induced wave polarized in the y direction.

9,2643E-08	1,4118E-07	1,19148E-07	1,14759E-07	1,42669E-07	1,2338E-07	1,61888E-07	1,67001E-07
1,21327E-07	1,03603E-07	7,54076E-08	1,70873E-07	1,42516E-07	1,071E-07	1,95878E-07	1,87726E-07
8,33059E-08	1,01716E-07	9,73619E-08	8,4846E-08	1,01026E-07	1,03269E-07	1,01673E-07	1,05778E-07
1,87879E-07	1,13543E-07	1,58064E-07	1,90969E-07	1,92631E-07	1,20444E-07	1,14337E-07	1,7877E-07
1,47728E-07	1,7029E-07	1,67322E-07	1,59575E-07	1,58673E-07	1,61997E-07	1,60349E-07	1,56597E-07
1,40409E-07	1,60155E-07	1,42067E-07	1,58204E-07	1,65118E-07	1,38599E-07	1,54419E-07	1,6401E-07

Table 9: fit parameter B from data from the opposite side from where the wave was induced, with the induced wave polarized in the y direction.

1,02E-05	1,03E-05	1,04E-05	1,05E-05	1,06E-05	1,07E-05	1,09E-05	1,11E-05
1,02E-05	1,03E-05	1,03E-05	1,05E-05	1,06E-05	1,07E-05	1,09E-05	1,1E-05
1,02E-05	1,03E-05	1,04E-05	1,05E-05	1,06E-05	1,07E-05	1,09E-05	1,1E-05
1,02E-05	1,03E-05	1,04E-05	1,04E-05	1,06E-05	1,07E-05	1,09E-05	1,1E-05
1,02E-05	1,03E-05	1,03E-05	1,05E-05	1,06E-05	1,07E-05	1,08E-05	1,1E-05
1,02E-05	1,03E-05	1,04E-05	1,05E-05	1,06E-05	1,07E-05	1,09E-05	1,11E-05

Table 10: standard deviation for fit parameter B from data from the opposite side from where the wave was induced, with the induced wave polarized in the y direction.

1,73076E-07	1,88769E-07	1,87665E-07	2,08171E-07	2,05318E-07	3,25986E-07	2,37142E-07	2,32789E-07
1,88926E-07	3,60512E-07	1,60227E-07	2,42613E-07	2,40118E-07	1,98318E-07	2,52146E-07	2,41117E-07
1,64898E-07	1,75207E-07	1,68387E-07	1,59057E-07	1,78302E-07	1,80576E-07	1,8234E-07	1,86665E-07
2,40533E-07	2,06581E-07	2,26001E-07	2,42465E-07	2,3118E-07	2,08757E-07	2,06719E-07	2,30029E-07
2,34389E-07	2,3368E-07	2,28255E-07	2,27051E-07	2,42556E-07	2,25671E-07	2,24415E-07	2,40906E-07
2,34845E-07	2,39569E-07	2,353E-07	2,46975E-07	2,29756E-07	2,20338E-07	2,41737E-07	2,31907E-07

Table 11: fit parameter C from data from the opposite side from where the wave was induced, with the induced wave polarized in the y direction.

2,52E-06	1,99E-06	2,25E-06	2,35E-06	1,98E-06	2,91E-06	1,9E-06	1,85E-06
2,23E-06	3,51E-06	2,9E-06	1,96E-06	2,3E-06	2,53E-06	1,75E-06	1,75E-06
2,66E-06	2,41E-06	2,46E-06	2,6E-06	2,45E-06	2,38E-06	2,4E-06	2,32E-06
1,66E-06	2,35E-06	1,86E-06	1,6E-06	1,53E-06	2,19E-06	2,26E-06	1,62E-06
1,96E-06	1,71E-06	1,74E-06	1,82E-06	1,82E-06	1,7E-06	1,73E-06	1,8E-06
2,14E-06	1,93E-06	2,08E-06	1,93E-06	1,82E-06	2,02E-06	1,88E-06	1,72E-06

Table 12: standard deviation for fit parameter C from data from the opposite side from where the wave was induced, with the induced wave polarized in the y direction.

2,91131E-07	2,8696E-07	2,98858E-07	3,24033E-07	3,0822E-07	5,49546E-07	3,43603E-07	3,31962E-07
2,92703E-07	6,40195E-07	2,62819E-07	3,51097E-07	3,69076E-07	3,0454E-07	3,52245E-07	3,36771E-07
2,61323E-07	2,70887E-07	2,51706E-07	2,42839E-07	2,65142E-07	2,65055E-07	2,67589E-07	2,74782E-07
3,35809E-07	3,12474E-07	3,21417E-07	3,35019E-07	3,17694E-07	3,07588E-07	3,05283E-07	3,16149E-07
3,39927E-07	3,21795E-07	3,21653E-07	3,20972E-07	3,46112E-07	3,15657E-07	3,1286E-07	3,40689E-07
3,4402E-07	3,49964E-07	3,49018E-07	3,6087E-07	3,18731E-07	3,11802E-07	3,41024E-07	3,18503E-07

Table 13: fit parameter A from data from the opposite side from where the wave was induced, with the induced wave polarized in the z direction.

5,57384E-06	5,56695E-06	5,52774E-06	5,46225E-06	5,38965E-06	5,26522E-06	5,16363E-06	4,9276E-06
5,65684E-06	5,65762E-06	5,61071E-06	5,50081E-06	5,44036E-06	5,35469E-06	5,23709E-06	5,22688E-06
5,62044E-06	5,62551E-06	5,51078E-06	5,51296E-06	5,41123E-06	5,26556E-06	5,2779E-06	5,08152E-06
5,48558E-06	5,47816E-06	5,41079E-06	5,3648E-06	5,30273E-06	5,17597E-06	5,06377E-06	5,06124E-06
5,32869E-06	5,32828E-06	5,25746E-06	5,15351E-06	5,09312E-06	4,96522E-06	4,96711E-06	4,85736E-06
4,80945E-06	4,82502E-06	4,80045E-06	4,72082E-06	4,60882E-06	4,56491E-06	4,39124E-06	4,41241E-06

Table 14: standard deviation for fit parameter A from data from the opposite side from where the wave was induced, with the induced wave polarized in the z direction.

3,49777E-07	3,55869E-07	3,50342E-07	3,40419E-07	3,34586E-07	3,25808E-07	3,12833E-07	2,84374E-07
3,53326E-07	3,54391E-07	3,47302E-07	3,35123E-07	3,34535E-07	3,26165E-07	3,17979E-07	3,09229E-07
3,54502E-07	3,52241E-07	3,39836E-07	3,42942E-07	3,31393E-07	3,19951E-07	3,05917E-07	2,88627E-07
3,88588E-07	3,72127E-07	3,47263E-07	3,41651E-07	3,36276E-07	3,23223E-07	3,10544E-07	2,99748E-07
3,65302E-07	3,60338E-07	3,58801E-07	3,46348E-07	3,39757E-07	3,30493E-07	3,19565E-07	3,13461E-07
3,1721E-07	3,16869E-07	3,15674E-07	3,06417E-07	3,02842E-07	2,85065E-07	2,7201E-07	2,69423E-07

Table 15: fit parameter B from data from the opposite side from where the wave was induced, with the induced wave polarized in the z direction.

1,02E-05	1,03E-05	1,04E-05	1,05E-05	1,06E-05	1,07E-05	1,09E-05	1,11E-05
1,02E-05	1,03E-05	1,03E-05	1,05E-05	1,06E-05	1,07E-05	1,09E-05	1,1E-05
1,02E-05	1,03E-05	1,04E-05	1,05E-05	1,06E-05	1,07E-05	1,09E-05	1,1E-05
1,02E-05	1,03E-05	1,04E-05	1,04E-05	1,06E-05	1,07E-05	1,09E-05	1,1E-05
1,02E-05	1,03E-05	1,03E-05	1,05E-05	1,06E-05	1,07E-05	1,08E-05	1,1E-05
1,02E-05	1,03E-05	1,04E-05	1,05E-05	1,06E-05	1,07E-05	1,09E-05	1,11E-05

Table 16: standard deviation for fit parameter B from data from the opposite side from where the wave was induced, with the induced wave polarized in the z direction.

6,80754E-08	6,78458E-08	6,87505E-08	6,85495E-08	6,86668E-08	6,95005E-08	6,82746E-08	6,79046E-08
6,59892E-08	6,54618E-08	6,62186E-08	6,52143E-08	6,66963E-08	6,62356E-08	6,69155E-08	6,41401E-08
6,5963E-08	6,47038E-08	6,54237E-08	6,66982E-08	6,63259E-08	6,65384E-08	6,27442E-08	6,13396E-08
7,45002E-08	7,06248E-08	6,74232E-08	6,75311E-08	6,62631E-08	6,71168E-08	6,58701E-08	6,27644E-08
6,9457E-08	6,88327E-08	7,03301E-08	7,05298E-08	6,99386E-08	7,15101E-08	6,80484E-08	6,79485E-08
7,07941E-08	7,05512E-08	7,05095E-08	7,16118E-08	7,1298E-08	7,02106E-08	7,05866E-08	6,90331E-08

Table 17: fit parameter C from data from the opposite side from where the wave was induced, with the induced wave polarized in the z direction.

1,12E-06	1,11E-06	1,12E-06	1,14E-06	1,15E-06	1,16E-06	1,16E-06	1,22E-06
1,09E-06	1,09E-06	1,1E-06	1,11E-06	1,12E-06	1,12E-06	1,14E-06	1,11E-06
1,09E-06	1,08E-06	1,1E-06	1,1E-06	1,11E-06	1,12E-06	1,1E-06	1,13E-06
1,06E-06	1,05E-06	1,09E-06	1,09E-06	1,1E-06	1,11E-06	1,12E-06	1,11E-06
1,05E-06	1,07E-06	1,06E-06	1,09E-06	1,09E-06	1,1E-06	1,07E-06	1,09E-06
1,11E-06	1,12E-06	1,12E-06	1,14E-06	1,13E-06	1,16E-06	1,17E-06	1,19E-06

Table 18: standard deviation for fit parameter C from data from the opposite side from where the wave was induced, with the induced wave polarized in the z direction.

9,66E-08	9,7E-08	9,68E-08	9,58E-08	9,71E-08	9,77E-08	9,65E-08	9,58E-08
9,32E-08	9,24E-08	9,21E-08	9,13E-08	9,36E-08	9,39E-08	9,51E-08	9,07E-08
9,2E-08	9,13E-08	9,11E-08	9,22E-08	9,19E-08	9,31E-08	8,7E-08	8,66E-08
1,17E-07	1,1E-07	9,72E-08	9,79E-08	9,73E-08	9,4E-08	9,27E-08	8,85E-08
1E-07	9,43E-08	9,98E-08	9,62E-08	9,58E-08	9,83E-08	9,3E-08	9,4E-08
9,87E-08	9,85E-08	9,86E-08	9,88E-08	1E-07	9,77E-08	9,87E-08	9,71E-08

C Appendix C COMSOL Multiphysics® simulation parameters

name	Value	description
Amp	1,00E-10	Maximum wave amplitude
c_long	5630[m/s]	longitudinal wave velocity
c_shear	2960[m/s]	shear wave velocity
c_trans	2640[m/s]	flexural wave velocity
D	0.1[mm]	Depth of the plate
data	40	data per pulz
dw	0[mm]	transducer offset
f	2 [MHz]	Frequency
L	40[mm]	Length of the plate
labda_c_long	c_long/f	P-Wave-Length
labda_c_shear	c_shear/f	S-Wave-Length
labda_c_trans	c_trans/f	Flex-Wave-Length
long	round(1.5*L/max_mesh)	number of mesh element for the long side
max_mesh	labda_c_long/8	maximum mesh element size
Mw	W/4	width of the middle rectangle of the transducer
tend	4/f0	time for dat data points
timelimit	1500*timestep	Timelimit of the simulation
timestep	tend/data	Time step
W	20[mm]	Width of the plate
wide	round(2*W/max_mesh)	number of mesh element for the wide side